STUDY OF STRUCTURAL AND OPTICAL PROPERTIES OF NiO-CuO NANOCOMPOSITE

Abstract

A new NiO-CuO nanocomposite has been successfully synthesized through a sol-gel method utilizing nickel chloride hexahydrate, copper chloride hexahydrate, ammonia, and ethylene glycol as precursors. The resulting material underwent comprehensive characterization using XRD, SEM, TEM, EDAX, UV–Visible, FTIR, and TGA-DTA techniques.

The XRD analysis revealed the presence of all pertinent Bragg's reflections, indicating a face-centered cubic and monoclinic structure for the NiO-CuO nanocomposite. The average particle size, determined using the Scherrer equations, was found to be 25 nm. Remarkably, this particle size value obtained from XRD was consistent with the results obtained from SEM and TEM analyses. The direct optical band gap of the nanocomposite was measured at 3.3 eV.

Furthermore, the thermal behavior of the mixed salts was examined through thermal analysis techniques (TG and DTA). To verify the purity of the composites and the elemental composition of the constituent oxides, FTIR and EDS analyses were performed.

Keywords: Sol-gel; Metal Oxide; Nanocomposite; semiconductors; Thermal

Authors

B. S. Satavekar
Department of Chemical Engineering
Tatyasaheb Kore Institute of Engineering and Technology
Warananagar, MS-India.

S. V. Anekar
Department of Chemical Engineering
Tatyasaheb Kore Institute of Engineering and Technology
Warananagar, MS-India.

B. S. Shirke
Department of Chemistry
Yashwantrao Chavan Warana Mahavidyalaya
Warananagar, MS-India.

I. INTRODUCTIONS

Now a day, the research in materials science is very active. Material science finds widespread application in engineering, technology and science. These materials include ceramics, polymers, semiconductors, magnetic materials and biomaterials etc. Nanotechnology is a rapidly emerging scientific subject in materials science that produces and constructs gadgets that are valuable to society for technical improvement [1]. Nanomaterials have special qualities include enhancing the electrical conductivity, ductility, toughness, and formability of ceramics, enhancing the hardness and strength of metals and alloys, and enhancing the luminous efficiency of semiconductors. It utilized to produce lightweight industrial applications with a high surface area to volume ratio, enhancing the functionality of electronics and information technology, enabling the use of more sustainable energy sources, and playing a crucial role in environmental remediation applications [2].

A composite material is characterized by its composition of at least two phases with differing chemical compositions. In the realm of nanotechnology, metal-polymer or metal oxide-polymer nanocomposites have emerged as a prominent category of materials. Theoretical and practical considerations surrounding these materials have been particularly intriguing. These materials offer the possibility of combining their properties to achieve desired responses. The alteration of optical or magnetic characteristics becomes especially noteworthy when particle sizes are drastically reduced. Such attributes hold significant appeal within the field of nanocomposite materials.

Composites exhibit a range of exceptional properties, including high hardness, a high melting point, low density, a low coefficient of thermal expansion, high thermal conductivity, excellent chemical stability, and enhanced mechanical properties such as increased specific strength, improved wear resistance, and specific modulus. These qualities position composites as promising candidates for diverse industrial applications, including the fields of sensors and energy conversion[3].

The performance of hybrid nanostructured materials hinges primarily on factors like their size, shape, composition, structure, and crystal phases. To attain the desired size, shape, and structure of hybrid nanostructures, it is imperative to master the controlled synthesis of these hybrid metal oxide nanostructures [4]. Various methods are available for creating nanocomposites, including homogeneous precipitation, co-precipitation, thermal decomposition, and hydrothermal processes. Among these methods, the sol-gel approach has found extensive application in the preparation of inorganic oxide nanocomposites [5]. While the conventional method for oxide preparation typically follows the ceramic route, the sol-gel route offers a range of advantages, including excellent homogeneity, a streamlined process, ease of remote operation, lower sintering temperatures, and more [6].

Nanoscale transition metal oxide semiconductors are very much in demand, due to their physical, biological, and chemical properties. This increases their application in a number of modern science and technology disciplines, as well as their ability to improve the environment and human health [7]. Mixed transition metal oxide (MTMO) has gained popularity in recent years as a potential material for numerous applications in electro catalysis, sensing, charge storage, and catalysis. The active surface area and charge transfer efficiency of MTMO nanocomposites are increased, which enhances the electrochemical

performance [8]. The development of metal oxide nanoparticles using green synthesis techniques is the subject of current study, which also offers a low-cost, economical method [9]. Researchers have looked into mixed catalysts in heterogeneous catalysis, which may be more effective than their individual parts [10].

Cupric oxide (CuO) is an inherently p-type semiconductor with a small band gap spanning from 1.2 eV to 3.57 eV among the several transition metal oxides. Its monoclinic structure and exceptional qualities—like its high stability, photovoltaic capabilities, super thermal conductivity, and antibacterial activity—make it distinctive. Photodetectors, photocatalysis, gas sensors, and solar cells are only a few of the many uses for CuO [11–13].

Nickel oxide (NiO) is a green crystalline solid that exhibits ferromagnetic properties and has a Neel temperature of 523 K. NiO nanostructures are categorized as p-type semiconductors and display unique magnetic and electrical characteristics that are dependent on particle size. This semiconductor material has a band gap ranging from 3.6 to 4.0 eV and is known for its exceptional chemical stability. Thanks to its affordability and remarkable ion storage capabilities, NiO has gained prominence as a compelling subject of research [14-16].

Numerous accounts in the literature detail the preparation of NiO-CuO powder using microwave processing. Samreen Zahra and colleagues unveiled that they successfully incorporated crystals of NiO and CuO nanoparticles, forming spheres of varying sizes, into an amorphous silica matrix consisting of agglomerated silica particles that coalesce to create clusters [17]. Sujit Chatterjee et al. highlighted the potential to reduce particle dimensions and enhance porosity through appropriate modifications of the synthesis method, leading to more efficient devices [18]. L. Argueta-Figueroa emphasized the viability of alternative, cost-effective metal oxide materials, including nickel oxide (NiO), copper oxide (CuO), manganese oxide, and cobalt oxide, as substitutes for expensive noble metals like gold (Au), platinum (Pt), lead (Pb), and palladium (Pd). Among these economically advantageous metal oxides, NiO and CuO are particularly noteworthy due to their favorable electrochemical stability and activity [19].

In the present study, we synthesized NiO-CuO nanocomposite by cost effective sol-gel route and characterized using techniques XRD, SEM, TEM, EDS, UV-DRS, TGA and FT-IR.

II. EXPERIMENTAL DETAILS

1. **Materials and Chemicals:** All chemicals used in this experiment were of reagent grade and used without any further purification. Nickel chloride hexahydrate ($NiCl_2.6H_2O$), copper chloride hexahydrate ($CuCl_2.6H_2O$), ammonia ($NH_4.OH$) and ethylene glycol procured from Sigma Aldrich were used as the precursors. All the glasswares which were utilized appropriately cleaned afterwards washed with distilled water. Deionized water has been used as the solvent throughout the synthesis.

2. **Synthesis of NiO-CuO Nanocomposites:** CuO-doped NiO nanocomposites were synthesized following the formula NiO-CuO (NixCu1-x (X = 0.1). The procedure involved blending the appropriate quantities of precursor solutions (0.1M) and gradually introducing aqueous ammonia (0.1M) while stirring continuously to achieve a pH level of

10-11. Once the pH was appropriately adjusted, the resulting green precipitate was rinsed with deionized water to eliminate byproducts formed during the reaction. After reaching a neutral solution, it was subjected to drying at 100°C for 24 hours. Subsequently, the particles were finely ground into a powder using an agate pestle and mortar, followed by thorough drying. The fine powder was then annealed at 400°C for 4 hours to produce NiO-CuO nanocomposites.

3. **Characterization of Nanocomposite Material:** Using a Siemens D-500 diffractometer with Cu-Kα (λ = 1.5406 Å) and running at 45 kV and 100 mA, the X-ray diffraction of the powder materials was measured throughout a 2θ angle range of 10^{o} to 80^{o}, at a scanning rate of 5°/min. A "Jasco (model V-770) UV-Vis-NIR Spectrophotometer" was used to record the UV-Visible (UV-Vis) absorption spectra, with a wavelength range of 200 to 800 nm. The powder sample was studied using a Transmission Electron Microscope (TEM) type, JEOL JEM 2100 plus, manufactured in Japan. Using the SDT Q600 model, manufactured by TA Instrument USA, data from thermogravimetric analysis, differential thermal analysis, and differential scanning calorimetry were acquired. A sample was subjected to Fourier transform infrared spectroscopy (FTIR) using the Agilent Technologies Cary 630 FTIR instrument.

III. RESULT AND DISCUSSION

1. **X-ray Diffraction:** Crystalline structure of materials was identified by x-ray diffraction method. Figure.1 shows XRD pattern of sample, it clearly indicating the formation of crystalline NiO-CuO nanocomposite material. The diffraction peaks of NiO-CuO nanocomposite at 32.46°, 35.52°, 38.72°, 48.80°, 53.42°, 58.23°, 61.57°, 66.12°, 68.08°, and 72.35° closely match with the planes (110), (002), (111), (-202), (020), (202), (022), (-113), (-311) and (113) good agreement with (JCPDS No. 89–5899) corresponds to the end-centered monoclinic structure of CuO and the diffraction peaks at 37.19°, 43.23°, 62.80°, 75.24° and 79.28° closely match with the (111), (200), (220), (311) and (222) crystalline planes and were indexed to face-centered cubic structure of NiO as per the (JCPDS No. 78- 0429).

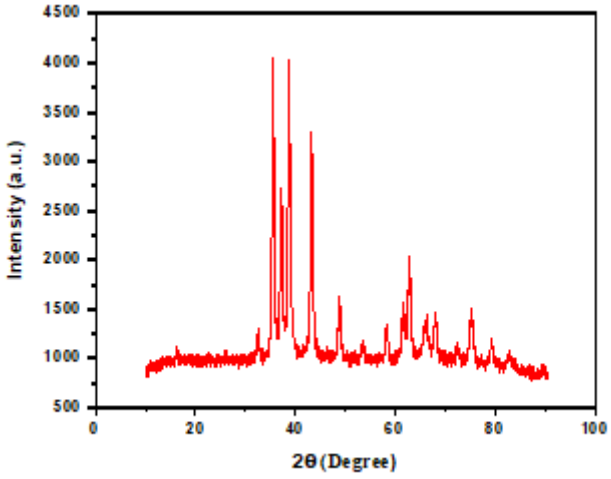

Figure 1: XRD pattern for of NiO-CuO nanocomposite

The impact of CuO nanoparticles on the microstructural characteristics of NiO: utilizing the following Scherrer equations, we have calculated the strain (ε) and average crystallite size (D) in the NiO sample based on the full width at half maximum (FWHM) of the XRD peaks:

$$D = \frac{k\lambda}{\beta\cos\theta}$$

$$\varepsilon = \frac{\beta\cos\theta}{4}$$

where, D is the average crystallite size, ε the strain , λ = 1.54056 Å is the wavelength of Cu kα, β is the full width at half-maximum intensity, θ is Bragg's diffraction angle, and K is a constant taken as to 0.94.

The values of D and ε estimated from XRD line width were about 25.26 nm and 0.24 % respectively for the NiO-CuO nanocomposites. The lattice constants comprising a, b, and c for the monoclinic structure, and a for the cubic structure were calculated using the following relationships, respectively.

$$\frac{1}{d^2} = \frac{1}{sin^2\beta}\left(\frac{\hbar^2}{a^2} + \frac{k^2 sin^2\beta}{b^2} + \frac{l^2}{c^2} - \frac{2\hbar l cos\beta}{ac}\right)$$

$$\frac{1}{d^2} = \left(\frac{\hbar^2 + k^2 + l^2}{a^2}\right)$$

The lattice parameters calculated from the present data are a =4.68 Å, b = 3.43 Å, and c = 5.14 Å for CuO, and a = 4.19 Å for NiO.

2. **Scanning Electron Microscopy (SEM):** The scanning electron microscopy (SEM) was employed to investigate the surface morphology, particle size distribution, and texture of the nanocomposite materials. Figure 2 displays the image of the nanocomposite synthesized through the sol-gel process. The image reveals that the particles are somewhat agglomerated, exhibiting a nanoflower-like morphology. The average particle size is approximately 25 nm. This morphological examination indicates that the material possesses a mesoporous structure, which in turn provides a greater number of active surface sites for adsorption. The particle size of the nanocomposites, as observed in the SEM images, aligns with the measurements derived from XRD analysis.

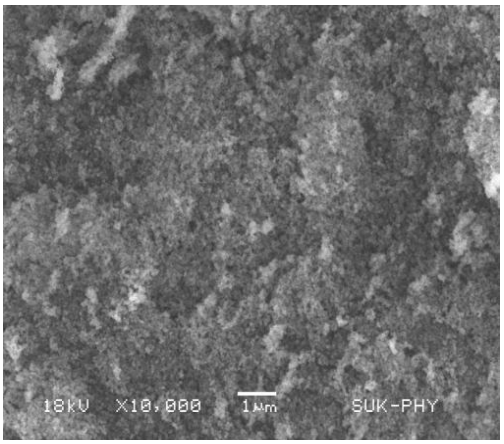

Figure 2: SEM image for of NiO-CuO nanocomposite

3. **Transmission Electron Microscopy (TEM):** Transmission electron microscopy (TEM) analysis provides valuable insights into the size and morphology of materials. Figure 3 presents a TEM image of the NiO-CuO nanocomposite, revealing both spherical and cubic structures within the material. The observed interconnections between nanoparticles indicate the formation of a mesoporous structure, with the nanoparticles aggregating in a spherical fashion. These results unambiguously demonstrate that the mean particle size obtained through TEM aligns well with the average crystallite size calculated from the XRD data, providing comprehensive information on the internal microstructure and crystallographic properties of the nanocomposites.

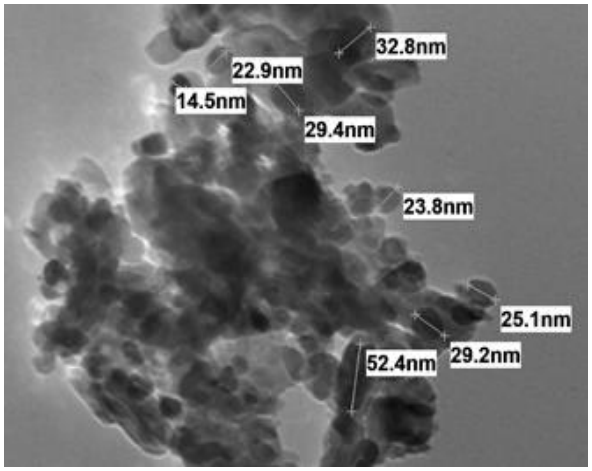

Figure 3: TEM image for of NiO-CuO nanocomposite

4. **Energy-dispersive X-ray Spectroscopy:** EDS analysis was employed to scrutinize the chemical composition of the synthesized samples, and the resulting EDS spectrum are displayed in Figure 4. The EDS spectrum of the NiO-CuO nanocomposite unequivocally affirms the presence of Ni, Cu, and O elements in the sample, with no indications of impurity peaks. Notably, the EDS spectrum illustrates a substantial oxygen content within the nanocomposites.

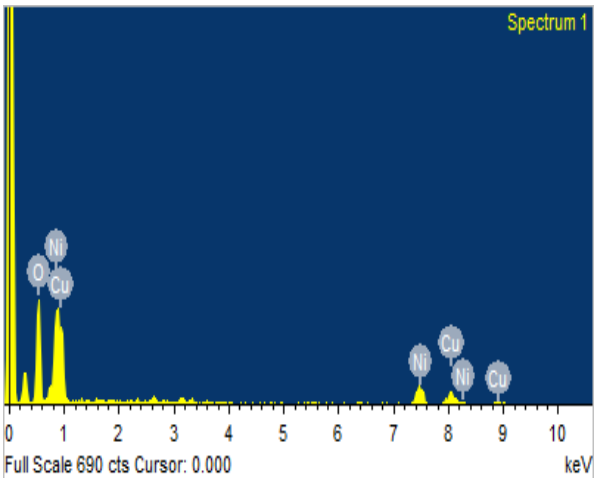

Figure 4: EDX image for of NiO-CuO nanocomposite

5. **UV–Vis DRS Spectral Study:** To determine the optical property of prepared nanocomposite, diffuse reflectance spectrum of the was investigated using UV-Visible optical spectroscopy in the range of 200 nm to 800 nm. It is shown in figure 5 a. Diffuse reflectance spectroscopy (DRS) analysis of absorbing material is based on Tauc formula as given below,

$$\alpha h\upsilon = B\,(h\nu - Eg)^{n}$$

In this equation, α (2.303A/d) represents the absorption coefficient, with A as the absorbance, d as the optical path length, B as the proportionality constant, Eg as the band gap energy, hυ as the energy of photons, and n as a constant. The value of the optical band gap for the prepared sample was determined through a Tauc plot, where $(\alpha h\upsilon)^2$ was plotted against (hυ). This analysis yielded a band gap energy of 3.3 eV, as illustrated in figure 5b.

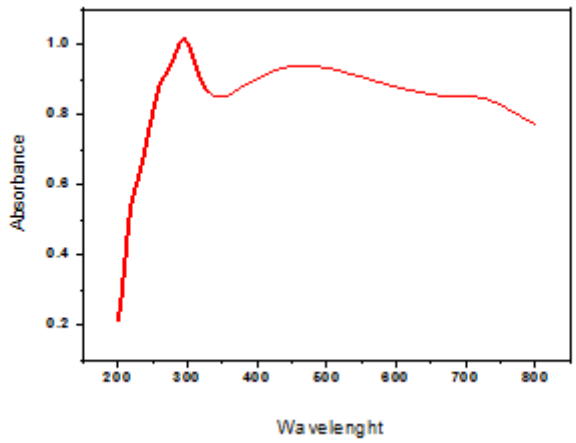

Figure 5: a. UV–Visible absorption spectrum of NiO-CuO nanocomposite

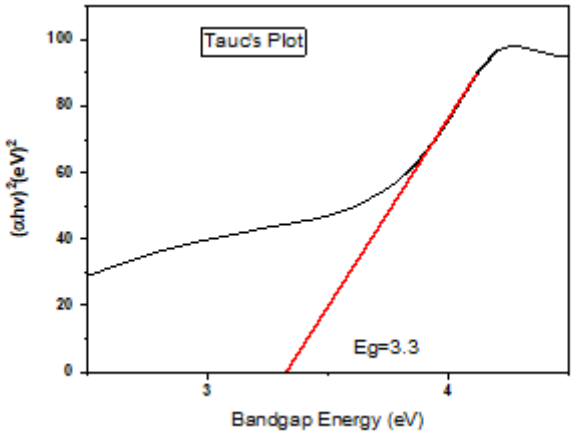

Figure 5: b. Tauc plot of NiO-CuO nanocomposite

6. **Fourier transform infrared spectroscopy (FTIR):** Fourier transform infrared spectroscopy (FTIR) was employed to detect the distinctive functional groups within the specimens. Figure 6 displays the FTIR spectrum of NiO-CuO composites. In the prepared sample, various absorption bands were observed across the spectral range of 400 cm^{-1} to 4000 cm^{-1}.

The O-H stretching exhibited a broad absorption peak at approximately 3443 cm^{-1}. The bands observed at 2922.78 and 2856.74 cm^{-1} were attributed to the bending vibrations of C-H bonds. Symmetric and asymmetric C=O stretching vibration modes were identified at 1629 cm^{-1} and 1387 cm^{-1}, respectively. Notably, the intensity of these peaks increased with higher Cu doping levels. A smaller peak at 801 cm^{-1} indicated C-H stretching, while the dip at 657 cm^{-1} represented vibrations of the metal-oxygen-metal bond. The presence of Cu-O bonds in the NiO-CuO nanocomposite was confirmed by a peak at 657.13 cm^{-1}. The stretching vibrational peak of NiO was a strong band at 482.40 cm^{-1}. The mixed oxides displayed a broad band ranging from 574.62 to 482.40 cm^{-1}, attributed to M-O vibrations. The broad nature of this band can be ascribed to the presence of nanoparticles in the mixed system.

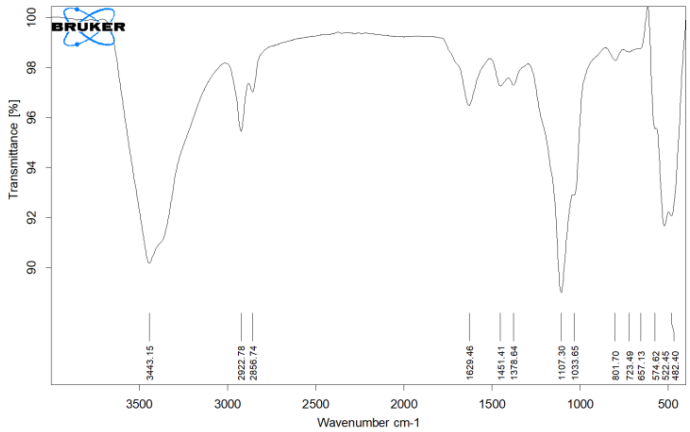

Figure 6: FTIR image of NiO-CuO nanocomposite

7. **Thermo Gravimetric Analysis (TGA):** To assess the thermostability of the NiO-CuO nanocomposite and study its oxidation and combustion characteristics, as well as perform kinetic analysis, differential scanning calorimetry (DSC), and thermo gravimetric analysis-differential thermal analysis (TGA-DTA) were conducted, as depicted in figure 7. TGA analysis was conducted under an air atmosphere, covering a temperature range from ambient temperature to 800°C.

Based on the TGA curve, the first step of evaporation occurred within the temperature range of 21°C to 159°C, with its peak at 60°C. This step resulted in a mass loss of approximately 0.7508%, equivalent to about 0.06466 mg. The second stage involved thermal decomposition within the temperature range of 159°C to 299.60°C, accompanied by a mass loss of about 0.8689%, approximately 0.07484 mg. In the third stage, desorption of two carbon dioxide and two nitrogen dioxide molecules occurred within the temperature range of 299.60°C to 337.94°C, leading to a mass loss of about 0.8689%, roughly 0.07484 mg. The fourth stage was characterized by the reduction of hydroxides to oxides through the loss of two water molecules, occurring between 337.94°C and 567°C, with a mass loss of about 0.4133%, approximately 0.03560 mg. The last thermal stability region, spanning from 567°C to 782°C, was defined as the region where residual polymer chains were incinerated.

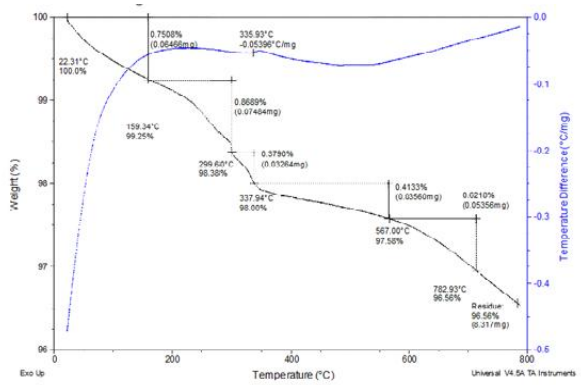

Figure 7: TGA/DSC image of NiO-CuO nanocomposite

IV. CONCLUSION

In summary, the NiO-CuO nanocomposite was successfully synthesized using the Sol-Gel method. The XRD pattern demonstrates the formation of a mixed coupled phase, comprising both cubic and monoclinic phases of NiO-CuO, with an average particle size of approximately 25 nm. SEM analysis revealed that an increase in the calcination temperature led to larger average crystallite size and enhanced agglomeration, primarily due to improved sample crystallinity. TEM analysis provided further insights, showcasing the presence of spherical and cubic structures within the NiO-CuO nanocomposite. Notably, the mean particle size determined by TEM closely matched the average crystallite size calculated from XRD data. Additionally, EDX spectra confirmed the presence of Ni, Cu, and O elements while revealing the absence of any impurity species. The UV-Visible study indicated the occurrence of both direct and indirect optical transitions. Furthermore, the study underscores the significant impact of incorporating CuO on the crystallite size and strain of NiO

nanoparticles. FTIR spectra affirmed the presence of CuO nanoparticles, with a notable peak observed at 657.13 cm−1 attributed to the Cu–O bond. Lastly, the thermal analysis of NiO-CuO, including oxidation and combustion behavior, was conducted, along with subsequent kinetic analysis, through the utilization of differential scanning calorimetry (DSC) and thermo gravimetric analysis-differential thermal analysis (TGA-DTA).

V. ACKNOWLEDGMENTS

The authors are gratefully acknowledges to the Institute of Tatyasaheb Kore Institute of Engineering and Technology Warananagar, and Yashwantrao Chavan Warana Mahavidyalaya, Warananagar, Maharashtra, India for providing laboratory facilities.

REFERENCES

[1] U. J. Tupe, M. S. Zambare, A. V. Patil and P. B. Koli, "The Binary Oxide NiO-CuONanocomposite Based Thick Film Sensor for the Acute Detection of Hydrogen Sulphide Gas Vapours," Mat. Sci. Res. India, 2020, Vol. 17(3), pp. 260-269.

[2] T. T. Bhosale, H. M. Shinde, N. L. Gavade, S. B. Babar, V. V. Gawade, S. R. Sabale · R. J. Kamble, B. S. Shirke, K. M. Garadkar, "Biosynthesis of SnO2 nanoparticles by aqueous leaf extract of Calotropisgigantea for photocatalytic applications," J. Mater. Sci. Mater. Electron, 2018, vol. 29(8).

[3] A. Sharma, S. Kumar, N. Budhiraja, S. Dahiya and Mohan, "Effect of calcination on optical properties and morphology of NiO-CuONanoComposites," Singh Arch. Appl. Sci. Res., 2013, vol.5 (3), pp.122-128.

[4] K. Ghanbari, Z. Babaei, "Fabrication and characterization of non-enzymatic glucose sensor based on ternary NiO/CuO/polyanilinenanocomposite," Analytical Biochemistry,2016.

[5] B. S. Shirke , A. A. Patil , P. P. Hankare , K. M. Garadkar, "Synthesis of cerium oxide nanoparticles by microwave technique using propylene glycol as a stabilizing agent," J. Mater. Sci: Mater Electron. 2011, vol. 22, pp. 200–203.

[6] K. M. Garadkar, B. S. Shirke, Y. B. Patil and D. R. Patil, "Nanostructured ZrO2 Thick Film Resistors as H2-Gas Sensors Operable at Room Temperature," Sensors & Transducers J., 2009, vol.110(11), pp.17-25.

[7] P. Mallick, C. S. Sahoo, "Effect of CuO Addition on the Structural and Optical Properties of NiO Nanoparticles," Nanoscience and Nanotechnology, 2013, vol. 3(3), pp.52-55.

[8] A.O. Juma, E.A.Arbab, C.M. Muiva, L.M. Lepodise, G.T. Mola, "Synthesis and characterization of CuO-NiO-ZnO mixed metal oxide nanocomposite," J. Alloy.Comp., 2017.

[9] T. T. Bhosale, A. R. Kuldeep, S. J. Pawar, B. S. Shirke, K. M. Garadkar, "Photocatalytic degradation of methyl orange by Eu doped SnO2 nanoparticles," J.Mat. Sci. Mat. Elect. 2019, vol. 30(20), pp.18927-18935.

[10] Abd El-Aziz A.Said, Mohamed M. Abd El-Wahab, Soliman A. Soliman, Mohamed N. Goda "Synthesis and Characterization of Nano CuO-NiO Mixed Oxides," Nanoscience and Nanoengineering 2014, vol. 2(1), pp.17-28.

[11] G. K. Weldegebrieal, "Photocatalytic and antibacterial activity of CuO nanoparticles biosynthesized using Verbascumthapsus leaves extract," Optik-International J.Light and Electron Optics, 2020, vol. 204, pp.164230.

[12] T. H. Tran and V. T. Nguyen, "Copper Oxide Nanomaterials Prepared by Solution Methods, Some Properties and Potential Applications: A Brief Review," International Scholarly Research Notices Volume 2014, Article ID 856592, pp.14.

[13] X. Zhao, P. Wang , Z. Yan, N. Ren, "Room temperature photoluminescence properties of CuO nanowire arrays," J. Opt. Mater. 2015, vol.42, pp.544-547.

[14] M. Bonomo, "Synthesis and Characterization of NiO Nanostructures: a Review "J.Nanoparticle Res 2018, vol.20(8), pp.222.

[15] A. Rahdar, M. Aliahmad and Y. Azizib, "NiO Nanoparticles: Synthesis and Characterization," JNS 2015, vol.5, pp.145-151.

[16] Shamim, Z. Ahmad, S. Mahmood, U.Ali, T. Mahmood and Z. Nizami, "Synthesis of nickel nanoparticles by sol-gel method and their characterization," Open J. Chem. 2019, vol. 2(1), pp.16-20.

[17] S. Zahra, N. Naz, M. Zia-ur-Rehman, M. Irfan, A. Sheikh andS.Izhar, "Characterization of Sol-gel Prepared Silica Supported NiO-CuO Composites," J. Chem. Soc. Pak., 2020, vol.42(2), pp.164-170.

[18] S. Chatterjee, A. Ray, M. Mandal, S. Das, and S. K. Bhattacharya,"Synthesis and Characterization of CuO-NiO Nanocomposites for Electrochemical Supercapacitors,"JMEPEG 2020, vol.29(12), pp.8036-8048.

[19] L. Argueta-Figueroa, "Synthesis, characterization and antibacterial activity of copper, nickel and bimetallic Cu–Ni nanoparticles for potential use in dental materials," Progress in Natural Science: Materials International 2014, vol.24(4), pp.321-328.

